

Casimir effect in rugby-ball type flux compactifications

Emilio Elizalde,^{1,*} Masato Minamitsuji,^{2,3,†} and Wade Naylor^{4,‡}

¹*Consejo Superior de Investigaciones Científicas, ICE/CSIC and IEEC, Campus UAB, Fac Ciències, 08193 Bellaterra (Barcelona) Spain*

²*ASC, Physics Department, LMU, Theresienstr. 37, Munich, Germany*

³*Yukawa Institute for Theoretical Physics, Kyoto University, Kyoto 606-8502, Japan*

⁴*Department of Physics, Ritsumeikan University, Kusatsu, Shiga 525-8577, Japan*

(Dated: June 11, 2018)

As a continuation of the work in [1], we discuss the Casimir effect for a massless bulk scalar field in a 4D toy model of a 6D warped flux compactification model, to stabilize the volume modulus. The one-loop effective potential for the volume modulus has a form similar to the Coleman-Weinberg potential. The stability of the volume modulus against quantum corrections is related to an appropriate heat kernel coefficient. However, to make any physical predictions after volume stabilization, knowledge of the derivative of the zeta function, $\zeta'(0)$ (in a conformally related spacetime) is also required. By adding up the exact mass spectrum using zeta function regularization, we present a revised analysis of the effective potential. Finally, we discuss some physical implications, especially concerning the degree of the hierarchy between the fundamental energy scales on the branes. For a larger degree of warping our new results are very similar to the ones given in Ref [1] and imply a larger hierarchy. In the non-warped (rugby-ball) limit the ratio tends to converge to the same value, independently of the bulk dilaton coupling.

PACS numbers: 04.50.+h;04.62.+v;98.80.Cq

Keywords: Extra dimensions, Quantum field theory

I. INTRODUCTION

Recent studies on braneworld models with extra dimensions that are compactified by a magnetic flux and bounded by codimension 2 branes (conical singularities) [2, 3] have revealed various fundamental properties, i.e., the regularization of branes (conical singularities)/linearized gravity [4, 5, 6] and stability against classical perturbations [7, 8]. There are still a lot of unsolved questions which should be clarified, especially concerning non-linear gravity and cosmology. Furthermore, careful analysis of these simpler models may give important physical insights on self-gravitating branes in various flux compactifications in string theory [9].

In this paper, we focus on models of braneworld based on a 6D supergravity [3], though we will work with its 4D counterpart [10], because of the lack of a formulation of the heat kernel coefficients for conical singularities in 6D. In these supergravity inspired models, the size of the compactified internal-space is not fixed classically and may behave as a volume modulus in a 4D effective theory. To fix this size of the volume (the volume modulus), we should therefore discuss other additional mechanisms. The authors of Ref. [1] focused on Casimir corrections for the case of perturbations of a massless, minimally coupled bulk scalar field. In this article, we present a revised analysis of the previous calculations, by performing a strict mode summation of the exact mass spectrum, which is now wholly taken into account.

We give an exact analysis of the one-loop effective action in a 4D alternative model. The one-loop effective potential for the volume modulus can be written in a form which is somewhat similar to the Coleman-Weinberg potential:

$$V_{4,\text{eff}} = \frac{A_4 - B_4 \ln(\mu^2 \rho_+)}{\rho_+}, \quad (1.1)$$

where ρ_+ characterizes the volume modulus and A_4 and B_4 are functions of the model parameters and the shape modulus (the degree of the warping of the bulk, which is completely determined if one fixes the brane tensions). Stability itself is determined by the sign of B_4 , which is closely related to the relevant heat kernel coefficients. However, to discern phenomenological effects on the brane, i.e., the effective mass of the modulus and the degree of

*Email: elizalde@ieec.uab.es

†Email: masato@theorie.physik.uni-muenchen.de

‡Email: naylor@se.ritsumei.ac.jp

the hierarchy between fundamental energy scales on the brane, we need to know the value of A_4 as well. A_4 is not just related to the heat kernel, although partly related with it; we also need to evaluate $\zeta'(0)$. Thus, an accurate evaluation of A_4 is crucial to make physical predictions, e.g., for the hierarchy or cosmological constant (CC) problems.

In the work [1], it has been shown how to divide A_4 into two parts, by introducing a continuous conformal transformation, going from the unwarped frame to the original warped geometry. The first part is associated with a one parameter family of conformal transformations and is called the cocycle function. This term can be obtained from heat kernel analysis. The second part consists of calculating the derivative of the zeta function in the unwarped frame, where to evaluate this piece we used the WKB approximation. In this paper we shall present an exact analysis of the mass spectrum for these *Kaluza-Klein* like modes in the unwarped frame.¹

The structure of the article is as follows: In the next section we briefly discuss our 4D analogue warped flux compactification model and review the tools to analyze the one-loop Casimir effect. We give the exact mass spectrum in the unwarped rugby-ball frame. In Sec. III we carry out the zeta function regularization in the unwarped frame. In Sec. IV, we give physical implications of our result, e.g., for the hierarchy problem by making comparisons with the results in [1]. We finish this article after giving a summary and some discussions.

II. 4D WARPED FLUX COMPACTIFICATION MODEL

Our main interest is the Casimir effect in the warped flux compactification model in 6D supergravity [3]:

$$S_6 = M_6^4 \int d^6x \sqrt{-g} \left(\frac{1}{2}R - \frac{1}{2}\partial_A\varphi\partial^A\varphi - \frac{1}{4}e^{-\varphi}F_{AB}F^{AB} - 2g_0^2e^\varphi \right), \quad (2.1)$$

where F_{AB} is the field strength of the electromagnetic field, φ is the dilaton, and g_0 is the bulk dilaton coupling. Hereafter, we set $M_6^4 = 1$ and if needed, we put it back explicitly. In order to evaluate the Casimir energy in this model, we need to know the heat kernel coefficients on the conical singularities. However, as mentioned in [1], there is no mathematical formulation of these coefficients the authors are aware of. Thus, in this paper, we focus on its 4D counterpart theory:

$$S_4 = M_4^2 \int d^4x \sqrt{-g} \left(R - \frac{1}{2}\partial_A\varphi\partial^A\varphi - \frac{1}{8}e^{-\varphi}F_{AB}F^{AB} - 4g^2e^\varphi \right), \quad (2.2)$$

which has a series of warped flux compactification solutions [10]

$$\begin{aligned} ds^2 &= h(\rho)d\theta^2 + \frac{d\rho^2}{h(\rho)} + (2\rho)(-d\tau^2 + dx_2^2), & h(\rho) &= \frac{2g^2}{\rho}(\rho_+ - \rho)(\rho - \rho_-), \\ \varphi(\rho) &= -\ln(2\rho), & F_{\theta\rho} &= -\frac{Q}{\rho^2}. \end{aligned} \quad (2.3)$$

We also set $M_4 = 1$ unless it is needed. Then, the branes correspond to strings, lying at the positions given by the *horizon-like* condition $h(\rho) = 0$. It is useful to define the coordinate $z = ((\rho_+ - \rho)/(\rho - \rho_-))^{1/2}$, to resolve the structure of spacetime in the case that $\rho_+ = \rho_-$. For $z \rightarrow 0, \infty$, there are cones whose deficit angles are obtained from the relation $\delta_\pm := 2\pi - g^2(\rho_+ - \rho_-)\Delta\theta/(\rho_\pm)$.

The moduli in the effective theory on the branes are characterized by ρ_\pm , or equivalently by ρ_+ and r , where the string tensions are related to the conical deficits by $\sigma_\pm = M_4^2\delta_\pm$. We stress that these relations are only valid for sufficiently small brane tensions, in comparison with the bulk scale M_4^2 . The coordinate θ is defined as $0 \leq \theta < \Delta\theta$ and $\Delta\theta$ is given by

$$\Delta\theta(r, \delta_+) = \frac{2\pi - \delta_+}{g^2(1-r)}, \quad (2.4)$$

where $r := \rho_-/\rho_+$. Once the brane tensions, σ_+ and σ_- are fixed, then r is also fixed and so we now regard as free parameters r and δ_+ , along with the dilaton bulk coupling g . The remaining degree of freedom used to determine the bulk geometry is the absolute size of the bulk, i.e., ρ_+ , which should be fixed by additional mechanisms.

¹ These modes are not the standard KK modes, because of the presence of conical singularities at the poles of the two-sphere on the internal dimensions. Given the similarity to a rugby ball we shall also call this unwarped frame the rugby-ball frame.

We discuss the basic properties of a massless, minimally coupled scalar field on this background:²

$$S_{\text{scalar}} = -\frac{1}{2} \int d^4x \sqrt{g} \phi \Delta_4 \phi. \quad (2.5)$$

Now consider a continuous conformal transformation of the metric, parameterized by ϵ ;

$$d\tilde{s}_{4,\epsilon}^2 = e^{2(\epsilon-1)\omega} ds_4^2, \quad \omega = \frac{1}{2} \ln(2\rho), \quad (2.6)$$

where for $\epsilon = 1$ we have the original metric, which we shall define as $\Delta_{4,\epsilon} = \Delta_4$, and $\epsilon = 0$ is the conformal frame. The classical action changes as

$$S_{\text{scalar}} = -\frac{1}{2} \int d^4x \sqrt{g} \phi \Delta_4 \phi = -\frac{1}{2} \int d^4x \sqrt{\tilde{g}} \tilde{\phi} \left(\tilde{\Delta}_4 + E_4(\epsilon) \right) \tilde{\phi}, \quad (2.7)$$

where

$$\begin{aligned} E_4(\epsilon) &= -(\epsilon-1)^2 \tilde{g}^{ab} \nabla_a \omega \nabla_b \omega + (\epsilon-1) \tilde{\Delta}_4 \ln \omega \\ &= \left(\frac{1}{2\rho} \right)^\epsilon \frac{g^2 (1-\epsilon) (\rho_+ - \rho_-) \{ \rho_+ (2 + (1-\epsilon)z^2) + \rho_- z^2 (-1 + \epsilon - 2z^2) \}}{(\rho_+ + \rho_- z^2)^2}. \end{aligned} \quad (2.8)$$

We now derive the mass spectrum in the unwarped frame:

$$\left(\tilde{\Delta}_4 + E(0) \right) \tilde{\phi}_\lambda = -\lambda^2 \tilde{\phi}_\lambda, \quad (2.9)$$

We shall decompose the mass eigenfunction as

$$\tilde{\phi}_\lambda = \int \frac{d^2k}{(2\pi)} \sum_{m,n} \Phi_\lambda(z) e^{in(2\pi/\Delta\theta)\theta} e^{i\mathbf{k}\mathbf{x}}. \quad (2.10)$$

The equation of motion of equation (2.9) has a series of exact solutions :

$$\begin{aligned} \Phi_\lambda(r) &= \sqrt{\frac{1+rz^2}{1+z^2}} \left[A \left(\frac{z^2}{1+z^2} \right)^{-n/2\kappa} \left(\frac{1}{1+z^2} \right)^{nr/2\kappa} {}_2F_1 \left(1-\nu - \frac{n}{2\kappa}(1-r), \nu - \frac{n}{2\kappa}(1-r), 1 - \frac{n}{\kappa}; \frac{z^2}{1+z^2} \right) \right. \\ &\quad \left. + B \left(\frac{z^2}{1+z^2} \right)^{n/2\kappa} \left(\frac{1}{1+z^2} \right)^{-nr/2\kappa} {}_2F_1 \left(1-\nu + \frac{n}{2\kappa}(1-r), \nu + \frac{n}{2\kappa}(1-r), 1 + \frac{n}{\kappa}; \frac{z^2}{1+z^2} \right) \right], \end{aligned} \quad (2.11)$$

where $\kappa := 1 - \frac{\delta_+}{2\pi}$.

$$\nu = \frac{1}{2} \left(1 + \sqrt{1 + \frac{\lambda^2 - k^2}{g^2} + \frac{n^2}{\kappa^2} (1-r)^2} \right). \quad (2.12)$$

Here we assume that the mode functions are regular on both conical boundaries. In order to ensure such a condition at $z = 0$ we must have $A = 0$ for $n > 0$ (and $B = 0$ for $n < 0$). Thus, we arrive at the following mass spectrum

$$\lambda^2 = k^2 + g^2 \left[4m(m+1) + \frac{2|n|}{\kappa} (2m+1)(1+r) + \frac{4n^2 r}{\kappa^2} \right], \quad m = 0, 1, 2, \dots \quad (2.13)$$

Note that this mass spectrum is very similar to the case of the gauge field perturbations [12]. (See also [6] for exact solutions of massless tensor perturbations).³

² A related model including a self-interaction term was discussed in [11].

³ Our method to determine the mass spectrum is essentially based on the same arguments as that in [12]. They impose two independent conditions, namely normalizability and regularity (denoted as ‘‘hermitian conditions’’ in [12]). However, if we were to only impose the condition of normalizability then there may still be other KK-type modes, though they are somewhat out of the scope of this paper.

From the above analysis, we can compare the results of the WKB approximation with this exact one. Note that the dependence on the winding number n appears only in the form of $|n|$. This fact just means that the internal space is axisymmetric. This mode sum will be the starting point for our analysis of the zeta function.

The coefficients in the one-loop effective potential, Eq. (1.1), can be written in the form

$$\begin{aligned}\int d^2x A_4(r, \delta_+) &= \int d^2\bar{x} \frac{A_4(r, \delta_+)}{\rho_+} = - \int_0^1 d\epsilon a_4(f = \frac{1}{2} \ln(\frac{2\rho}{\rho_+})) - \frac{1}{2} \zeta'(0, \Delta_4, \epsilon=0), \\ \int d^2x B_4(r, \delta_+) &= \int d^2\bar{x} \frac{B_4(r, \delta_+)}{\rho_+} = \frac{1}{2} \zeta(0, \Delta_4, \epsilon=0) = \frac{1}{2} a_4(f = 1),\end{aligned}\quad (2.14)$$

where the zeta function $\zeta(s)$ is defined for the given mass spectrum in the unwarped frame Eq. (2.13):

$$(2\pi)^2 \zeta(s) = \int d^2x \int d^2k \sum_{m,n} \lambda_{mnk}^{-2s}. \quad (2.15)$$

The coefficients other than $-\zeta'(0)/2$ in the conformal frame were derived in Ref. [1], where it was shown that the term $A_4(r, \delta_+)$ is given by the equation

$$A_4(r, \delta_+) = (A_4(r, \delta_+))_{\text{cocycle}} + (A_4(r, \delta_+))_{\text{unwarped}}, \quad (2.16)$$

where the first term is the cocycle correction. In the next section, we will discuss the evaluation of the second term, which is $-\zeta'(0)/2$ in the unwarped, factorizable frame:

$$\int d^2x (A_4(r, \delta_+))_{\text{unwarped}} = -\frac{1}{2} \zeta'(0, \Delta_4, \epsilon=0). \quad (2.17)$$

The cocycle function can be derived from heat kernel analysis [1]:⁴

$$\begin{aligned}A_{4,\text{cocycle}}(r, \delta_+) &= -\frac{g^2(2\pi - \delta_+)}{1440\pi^2} \int_0^1 d\epsilon \int_0^\infty dz \left(\frac{1}{2} \ln\left(\frac{2\rho}{\rho_+}\right) \right) \frac{z}{(1+z^2)(1+rz^2)} \frac{\Psi(1, r, \epsilon, z)}{(1+rz^2)^4} \\ &\quad - \frac{g^2}{144\pi} \frac{\delta_+}{2\pi} \frac{2 - \frac{\delta_+}{2\pi}}{1 - \frac{\delta_+}{2\pi}} \left[2 \ln(2) - 1 + r - \frac{1}{5} \frac{1 + (1 - \frac{\delta_+}{2\pi})^2}{(1 - \frac{\delta_+}{2\pi})^2} \left(\frac{1}{2} \ln(2)(1 - 3r) + \frac{1-r}{2} \right) \right] \\ &\quad - \frac{g^2}{144\pi} \frac{\frac{\delta_+}{2\pi} - (1-r)}{r} \frac{r + (1 - \frac{\delta_+}{2\pi})}{1 - \frac{\delta_+}{2\pi}} \\ &\quad \times \left[2 \ln(2r) - 1 + \frac{1}{r} - \frac{1}{5} \frac{r^2 + (1 - \frac{\delta_+}{2\pi})^2}{(1 - \frac{\delta_+}{2\pi})^2} \left(\frac{1}{2} \ln(2r)(1 - \frac{3}{r}) + \frac{1 - \frac{1}{r}}{2} \right) \right],\end{aligned}\quad (2.18)$$

where $\Psi(\rho_+, \rho_-, \epsilon, z)$ can be found in Appendix B of [1] and is just a function of r and z . The independence of Ψ on ϵ is discussed in [1]. The coefficient $B_4(r, \delta_+)$ is given by

$$B_4(r, \delta_+) = (B_4(r, \delta_+))_{\text{bulk}} + (B_4(r, \delta_+))_{\text{brane}}, \quad (2.19)$$

where

$$(B_4(r, \delta_+))_{\text{bulk}} = \frac{g^2(2\pi - \delta_+)}{1440\pi^2} \int_0^\infty dz \frac{z}{(1+z^2)(1+rz^2)} \frac{\Psi(1, r, 0, z)}{(1+rz^2)^4}, \quad (2.20)$$

and

$$\begin{aligned}(B_4(r, \delta_+))_{\text{branes}} &= \frac{g^2}{288\pi} \frac{\delta_+}{2\pi} \frac{2 - \frac{\delta_+}{2\pi}}{1 - \frac{\delta_+}{2\pi}} \left[4 - \frac{1}{5} \frac{1 + (1 - \frac{\delta_+}{2\pi})^2}{(1 - \frac{\delta_+}{2\pi})^2} (1 - 3r) \right] \\ &\quad + \frac{g^2}{288\pi} \frac{\frac{\delta_+}{2\pi} - (1-r)}{r} \frac{r + (1 - \frac{\delta_+}{2\pi})}{1 - \frac{\delta_+}{2\pi}} \left[4 - \frac{1}{5} \frac{r^2 + (1 - \frac{\delta_+}{2\pi})^2}{(1 - \frac{\delta_+}{2\pi})^2} (1 - \frac{3}{r}) \right],\end{aligned}\quad (2.21)$$

which is also derived from heat kernel analysis.

⁴ See also [13], for UV effects and heat kernel coefficients in higher dimensions.

III. ZETA FUNCTION REGULARIZATION IN THE UNWARPED CONFORMAL FRAME

Given the eigenvalues we found in the previous section, we shall now derive an expression for the corresponding spectral zeta function and related quantities, such as the effective action. In Ref [1] the authors used the density of states method because they had not found an exact mode spectrum.

The first step on our journey will be to use the Mellin transform:

$$\zeta(s) = \frac{1}{\Gamma(s)} \int d^2x \int d^2k \sum_{m,n} \int_0^\infty t^{s-1} \exp\{-[k^2 + g^2(a(m+\alpha)^2 + b(m+\alpha)|n| + cn^2 + q)]t\}, \quad (3.1)$$

where we have just rearranged the eigenvalue λ_{mnk} , see equation (2.13), such that it takes the form of a two dimensional Epstein zeta function, and

$$a = 4, \quad b = \frac{4(1+r)}{\kappa}, \quad c = \frac{4r}{\kappa^2}, \quad q = -1, \quad \alpha = 1/2. \quad (3.2)$$

Firstly, we perform the k -integration after interchanging the order of integrations:

$$\begin{aligned} \int d^2x \int d^2k \sum_{m,n} \lambda_{mnk}^{-2s} &= \frac{1}{\Gamma(s)} \int d^2x \int d^2k \sum_{m,n} \int_0^\infty dt t^{s-1} \exp\{-[k^2 + g^2(a(m+\alpha)^2 + b(m+\alpha)|n| + cn^2 + q)]t\} \\ &= \int d^2x \sum_{m,n} \frac{2\pi}{\Gamma(s)} \int_0^\infty dt t^{s-2} \exp\{-g^2[a(m+\alpha)^2 + b(m+\alpha)|n| + cn^2 + q]t\} \\ &= \int d^2x \frac{2\pi g^{2(1-s)}}{s-1} \sum_{m,n} [a(m+\alpha)^2 + b(m+\alpha)|n| + cn^2 + q]^{1-s} \end{aligned} \quad (3.3)$$

where in the third step we have redefined the terms such that

$$\begin{aligned} \hat{\alpha}(n) &= \alpha + \frac{bn}{2a} = \frac{1}{2} + \frac{(1+r)|n|}{2\kappa}, \\ \hat{q}(n) &= q + cn^2 - \frac{(bn)^2}{4a} = -\frac{n^2}{\kappa^2}(1-r)^2 - 1. \end{aligned} \quad (3.4)$$

This form shows that the zeta function is essentially some kind of two-dimensional Epstein zeta function as we show below. In the following discussion, we focus on the non-axisymmetric modes $n \neq 0$. For the contribution of the axisymmetric modes, see Appendix A.

A. Extended binomial expansion

Frequently, the form of the two-dimensional Epstein zeta function allows one to perform its summation in an elegant way which involves the Chowla-Selberg expansion formula or more frequently (as it would correspond to the case here) a generalization thereof, see [14]. However, some conditions must be fulfilled, in particular, the quadratic form must be positive definite and the constant q term should be also non-negative. But this is not here the case, and the fact that $q < 0$ does not allow for such a beautiful analysis. Henceforth, we shall apply in what follows what we have called the *extended binomial expansion* approach (see also [15]), namely, we will introduce an extra summation via

$$\begin{aligned} &\sum_{m=0}^{\infty} \sum_{n=1}^{\infty} [a(m+\alpha)^2 + b(m+\alpha)n + cn^2 + q]^{-s+1} \\ &= \sum_{m=0}^{\infty} \sum_{n=1}^{\infty} [a(m+\hat{\alpha})^2 + \hat{q}]^{-s+1} = \sum_{m=0}^{\infty} \sum_{n=1}^{\infty} \sum_{j=0}^{\infty} \frac{\Gamma(j+s-1)}{\Gamma(s-1)j!} [a(m+\hat{\alpha})^2]^{1-s-j} \hat{q}^j, \end{aligned} \quad (3.5)$$

where the validity of the binomial expansion is defined for

$$\left| \frac{\hat{q}}{a(m+\alpha)^2} \right| < 1, \quad (3.6)$$

which is indeed satisfied for all possible values of m and n in our model.

The crucial step is to interchange now the summation over j with the m, n summations. The absolute convergence of the binomial expansion in j guarantees such an interchange. Whence, we obtain that

$$\sum_{m=0}^{\infty} \sum_{n=1}^{\infty} [a(m+\alpha)^2 + b(m+\alpha)n + cn^2 + q]^{-s+1} = \sum_{j=0}^{\infty} \sum_{n=1}^{\infty} a^{1-s-j} \frac{\Gamma(j+s-1)}{\Gamma(s-1)j!} \hat{q}^j \zeta_H(2s+2j-2, \hat{\alpha}), \quad (3.7)$$

where we have summed over n to give a standard relation in terms of Hurwitz zeta functions. Substitution of the above relation into Eq. (3.3) leads to

$$\zeta(s)|_{n \neq 0} = \frac{g^{2(1-s)}}{\pi} \int d^2x \sum_{j=0}^{\infty} G(j, s) \sum_{n=1}^{\infty} \left(\frac{n^2}{\kappa^2} (1-r)^2 + 1 \right)^j \zeta_H \left(2s+2j-2, \frac{1}{2} + \frac{1+r}{2\kappa} n \right) \quad (3.8)$$

with

$$G(j, s) = \frac{2^{-2(j+s-1)} \Gamma(s+j-1)}{\Gamma(s)j!}. \quad (3.9)$$

Note also that the presence of $|n|$ in our mode sum, with $-\infty \leq n \leq \infty$, makes the zeta function a non-typical one. In our approach, we have just multiplied by two and taken the sum from $n = 1 \dots \infty$, the $n = 0$ mode having been treated independently.

The above expression does not converge unless $\text{Re } s \geq 3$ and thus, we must first analytically continue the zeta function in equation (3.8) in the usual way [17], by first subtracting off the terms responsible for the divergences in $\zeta(s)$. After this we are able to take the derivative at $s = 0$, being careful to add back the terms we subtracted off before the analytic continuation.

B. Analytic continuation of the ζ – function

In order to isolate the divergent behavior in the zeta function, due to small s , we need to make an asymptotic expansion of Eq. (3.8), the details of which are given in Appendix A. From this we can now analytically continue $\zeta(s)$ and take the derivative at $s = 0$. Subtracting off the divergent terms from the zeta function leads to a function

$$P(s) = \frac{g^{2(1-s)}}{\pi} \int d^2x \sum_{j=0}^{\infty} G(j, s) \sum_{n=1}^{\infty} \left[\left(\frac{n^2}{\kappa^2} (1-r)^2 + 1 \right)^j \zeta_H \left(2s+2j-2, \frac{1}{2} + \frac{1+r}{2\kappa} n \right) - F(n, j; s) \right], \quad (3.10)$$

where $P(s)$ is now a regular function at $s = 0$ and $F(n, j; s)$ is defined in Appendix A. Performing the sum over j and adding back the subtracted terms leads to the analytically continued zeta function

$$\zeta(s)|_{n \neq 0} = P(s) + \sum_{j=0}^{\infty} G(j, s) \Delta(j, s) \quad (3.11)$$

where, given that the subtracted terms are simple functions of n , they can be expressed as a combination of ordinary Riemann zeta functions:

$$\Delta(j, s) = \frac{g^{2(1-s)}}{\pi} \int d^2x \kappa^{1+2s} \frac{(1-r)^{2j}}{(1+r)^{1+2j+2s}} \frac{2^{-6+2j+2s}}{45(2s+2j-3)} \left[\frac{w_0}{\kappa^4} \zeta_R(2s-3) + \frac{w_2(j, s)}{\kappa^2} \zeta_R(2s-1) + w_4(j, s) \zeta_R(2s+1) \right], \quad (3.12)$$

the functions w_0, w_2 and w_4 being defined in Appendix A. Note, however, that we must leave the sum over n in $P(s)$ as it is. The $j = 0$ and $j = 1$ terms must be considered separately because of the gamma functions in $G(j, s)$ (see Eq. (3.9)), which leads to compensations of poles and zeros of the Riemann zeta functions in Eq. (3.12). Taking all of this into account, the analytic continuation of the derivative of $P(s)$ with respect to s can be found without any further problems.

Then, after analytic continuation to $s \rightarrow 0$, we obtain $P'(0)$ as given in Appendix B. In Fig. 1 we have plotted the function $P'(0)$ as a function of r . As can be seen, the summation over j converges fairly rapidly and the result for $j_{\max} = 10$ already coincides well with that for $j_{\max} = 50$. In the following calculations, we shall use $j_{\max} = 50$ as a conservative choice. Note that in all of our plots the n -summation converges fairly quickly due to the asymptotic expansion and the first few terms would suffice; however, we will always set $n_{\max} = 50$ as a conservative choice.

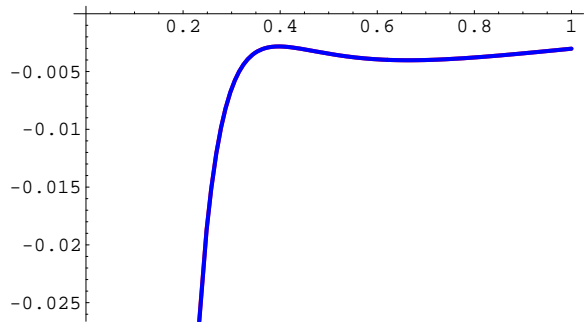


FIG. 1: Plots for $P'(0)$, Eq. (B2), as a function of r are shown for $\delta = 0.01$. The red and blue curves correspond to the truncation of the j -summation at $j_{\max} = 10$ and $j_{\max} = 50$, respectively.

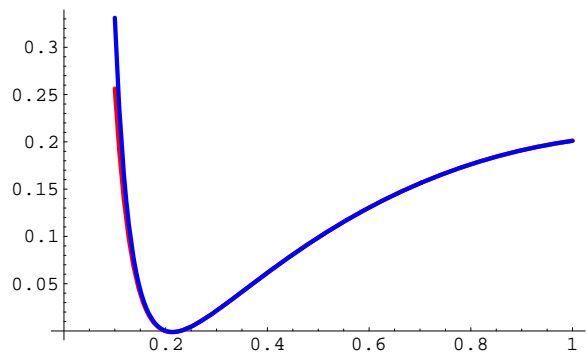


FIG. 2: Plots of the derivative $(d/ds)(\sum_j G\Delta)(s)|_{s=0}$, Eq. (3.13), as a function of r are shown for $\delta = 0.01$. The red and blue curves correspond to the truncation of the j -summation at $j_{\max} = 10$ and $j_{\max} = 50$, respectively.

The analytic continuation of the counterterms $\sum_j G(j, s)\Delta(j, s)$ is discussed in Appendix B, where after considering the $j = 0$, $j = 1$ and $j \geq 2$ modes separately we find (see App. B)

$$\frac{d}{ds} \sum_{j=0}^{\infty} \left(G(j, s)\Delta(j, s) \right) \Big|_{s=0} = \frac{d}{ds} \left(G(0, s)\Delta(0, s) \right) \Big|_{s=0} + \frac{d}{ds} \left(G(1, s)\Delta(1, s) \right) \Big|_{s=0} + \sum_{j=2}^{\infty} \frac{d}{ds} \left(G(j, s)\Delta(j, s) \right) \Big|_{s=0} \quad (3.13)$$

In Fig. 2 we plot Eq. (3.13) as a function of r . The j -summation truncated at $j_{\max} = 10$ already exhibits good convergence and coincides well with that for $j_{\max} = 50$. In the following calculations, we use $j_{\max} = 50$ as a conservative choice.

We finish this section by noting that the above, quite involved mathematics have yielded in the end very precise numerical results. We will now take advantage of them by considering their implication —e.g., those of the Casimir corrections from bulk fields— for the phenomenological predictions that were mentioned in the first section.

IV. IMPLICATIONS FOR THE HIERARCHY PROBLEM

We can now consider the physical implications on the brane in the original 6D theory given by Eq. (2.1). In Ref [1], several phenomenological applications have been discussed, i.e., to the hierarchy problem and the vacuum (Casimir) energy density (i.e., the effective 4D cosmological constant) on the branes. With our new results at hand, we give a revised version of them, especially focusing on the hierarchy problem. After analysing the hierarchy problem, we briefly discuss the case of the vacuum energy density.

In the original six-dimensional model, the *effective* four-dimensional Planck scale is

$$M_{\text{pl}}^2 \simeq \frac{\rho_+ (2\pi - \delta_+)}{g_0^2} M_6^4. \quad (4.1)$$

If we assume a brane localized field whose bare mass is given by m^2 on either brane at ρ_{\pm} then the observed mass scales are $m_+^2 = m^2$ and $m_-^2 = r^2 m^2$. Thus, the mass ratio between the field and the effective Planck mass is given by

$$\frac{m_{\pm}^2}{M_{\text{pl}}^2} \simeq \frac{\mu^2 m^2}{M_6^4} \frac{g_0^2}{2\pi - \delta_+} e^{-(2A_6 + B_6)/(2B_6)}, \quad (4.2)$$

where A_6 and B_6 correspond to A_4 and B_4 in the 6D model, respectively. Assuming the factor $(\mu m/M_6^2)^2$ takes an optimal value of $\mathcal{O}(1)$ at the unification of the fundamental scales, then the mass ratio becomes

$$\frac{g_0^2}{2\pi - \delta_+} e^{-(2A_6 + B_6)/(2B_6)}, \quad (4.3)$$

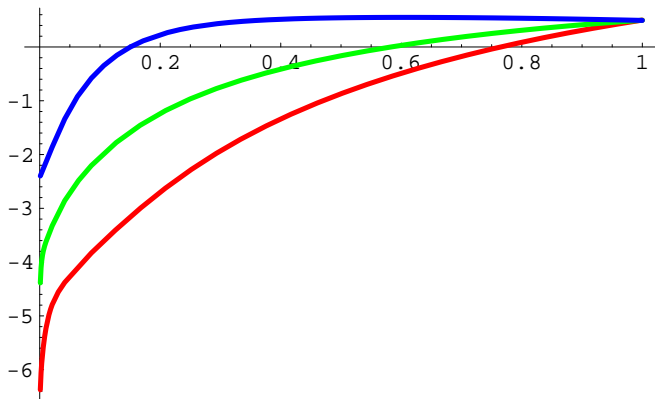


FIG. 3: Numerical plots of $\log_{10} R(r, \delta_+ = 0.01)$ as a function of r are shown for $g = 0.5, 5, 50$ (the red, green and blue curves, respectively). We set $j_{\max} = n_{\max} = 50$ as a conservative choice.

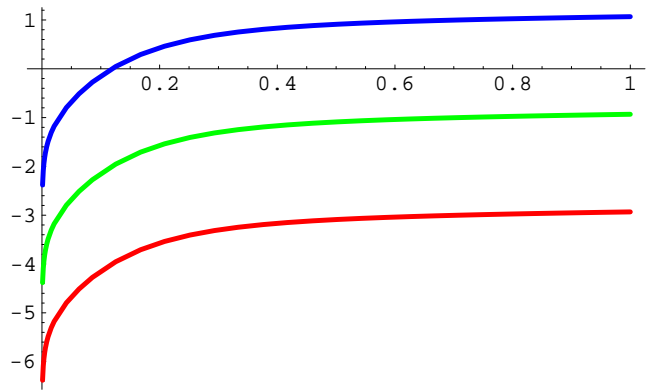


FIG. 4: Numerical plots of $\log_{10} R(r, \delta_+ = 0.01)$, via the WKB approximation, as a function of r are shown for $g = 0.5, 5, 50$ (red, green and blue curves, respectively).

where we have used the value of ρ_+ , at stabilization. The corresponding quantity in the 4D toy model is given by

$$R(r, \delta_+) = \frac{g^2}{2\pi - \delta_+} e^{-(A_4 + B_4)/B_4}. \quad (4.4)$$

In Fig. 3 we have plotted $\log_{10} [R(r, 0, 01)]$ as a function of r . The resulting ratios between the scalar and gravitational energies lead to the same conclusions as in the analysis given in Ref. [1], in which the derivative of the zeta function was evaluated by the WKB method (See Fig. 4). Namely, we obtain larger mass hierarchies for smaller r and smaller g ; in detail, however, the form of R is not the same. The most important difference is the behavior at $r = 1$: in the exact spectrum R does not depend on the coupling g (whereas in the WKB approximation it scales as g^2). Numerical plots also show that this feature is almost independent of the value of the deficit angle δ_+ . Thus, the expected mass hierarchy in the rugby-ball frame is independent of the value of the dilaton coupling g , which is actually the bulk cosmological constant, because the dilaton dynamics are absent in the conformal (rugby-ball) frame.

Finally, we add a few comments on the Casimir energy density realized on the branes, i.e., the effective 4D cosmological constant. As shown in Eq. (56) (also see (57)), the expression for the vacuum energy density has a very similar form to R , since $B_4(r, \delta_+) \propto g^2$. In fact, after setting $\mu = M_4$ as an optimal choice, numerical plots of Eq. (57) in Ref. [1] as a function of r for different dilaton coupling g again show convergence to the same point in the $r \rightarrow 1$ limit, though here we do not present these results explicitly. For smaller r , the same behavior as in Fig. 5 in [1] is obtained and implies a tiny amount of effective cosmological constant on the branes, in comparison with the gravitational energy scale M_4^2 . The only problem is that the sign of the energy density becomes negative, as is expected from the form of the effective potential Eq. (1.1). This fact requires an additional uplifting mechanism for the effective potential.

V. CONCLUSION

In this article, we have given a precise analysis of the mode summation in deriving the one-loop effective potential for the volume modulus in a 4D analogue model of a warped flux compactification based on 6D supergravity. In [1] the mass spectrum was found using the leading order WKB approximation. Strictly speaking, this is only an approximation and an exact one-loop analysis of the mass spectrum has been performed in the present paper, by employing zeta function regularization techniques. We would also like to stress that the unwarped frame is not the standard Kaluza-Klein spacetime, because of the presence of conical singularities.⁵

In this paper we used our results to look at the hierarchy problem in warped flux compactification models. The qualitative features in Fig. 3 are similar to those of Fig. 4: we expect a larger mass hierarchy for smaller r (where

⁵ A beautiful discussion of zeta function regularization in standard KK theories can be found in [15].

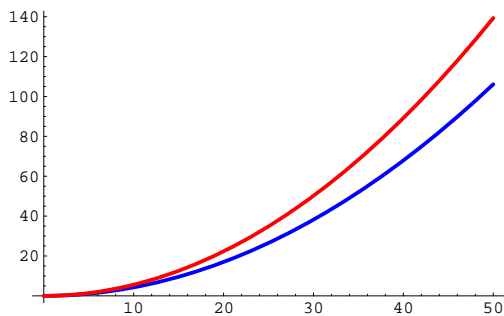


FIG. 5: Numerical plot of the integrand of $\zeta(0)$ and $2B_4$ as functions of g are shown for $r = 1$ and $\delta_+ = 0.01$. The red and blue curves correspond to the cases of $\zeta(0)$ and $2B_4$, respectively. We set $j_{\max} = n_{\max} = 50$.

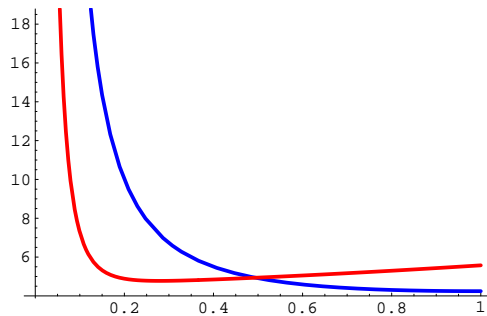


FIG. 6: Numerical plot of the integrand of $\zeta(0)$ and $2B_4$ as functions of r are shown for $g = 10$ and $\delta_+ = 0.01$. The red and blue curves correspond to the cases of $\zeta(0)$ and $2B_4$, respectively. We set $j_{\max} = n_{\max} = 50$.

r is the degree of warping) and for larger bulk dilaton coupling g . Indeed, for $r \ll 1$, the contribution from the cocycle function becomes important and gives rise to a large mass hierarchy on the brane, though at the same time the effective mass of the modulus may become lighter (and hence more unstable to KK perturbations). However, quantitatively there is a significant difference for $r \lesssim 1$, where quite surprisingly all the curves for different values of g in Fig. 3 converge to the same point at $r = 1$. In Fig. 4, which is for the WKB approximation, the behavior of R is proportional to g^2 , even at $r = 1$. This may well represent a non-trivial feature of the Casimir effect in the rugby ball limit. Similar results are obtained in the case of the vacuum (Casimir) energy density on the branes, namely convergence to the same value in the $r \rightarrow 1$ limit, independently of g . For smaller values of r , we can expect a tiny amount of the effective cosmological constant on the branes, in comparison with the gravitational energy scale. The negativity of the energy density may require slight modifications of the background model.

As a consistency check of our results, in Figs. 5 and 6 we have plotted the integrands of $\zeta(0)$ and $B_4(r, \delta_+)$, which are related to $a_4(f = 1)$ given in Eq. (2.14), as functions of g and r , respectively, for a fixed value of the deficit angle, δ_+ . Note that both quantities are practically insensitive to δ_+ . In the unwarped frame, due to the properties of the heat kernel coefficients (see e.g., [16]), the equation $\zeta(0) = a_4(f = 1)$ should be satisfied. Although they do not agree exactly, they do exhibit a similar behavior, namely increasing for larger g and for smaller r . We thus conclude that our results are physically reliable. Nevertheless, there are still slight differences between these values and it is worthwhile to consider the possible origin of this difference.

In [1] the authors confirmed that B_4 (and thus $a_4(f = 1)$) is independent of the value of ϵ [16], which characterizes the conformal transformation given in Eq. (2.6) and therefore, we believe that B_4 is correct.⁶ We have also carefully checked the convergence of the mode summations. Thus, it is the view of the authors that a possible origin for the disagreement could be in our determination of the exact mode spectrum. By imposing vanishing conditions for the mode functions and their derivatives at the poles (branes), we were able to derive the mass spectrum in the rugby-ball frame. Our method to determine the mass spectrum is essentially based on the same arguments given in [12], where two conditions, normalizability and regularity at the poles were imposed (more precisely, it was demanded that the wave functions should be Hermitian). However, if only normalizability were imposed, this would allow for logarithmic divergences at the poles and this may well lead to additional modes in the eigenvalue spectrum, which could then reflect in the differences between Figs. 5 and 6. Regardless of this, based on the qualitative behavior of B_4 and $\zeta(0)$, the existence of such modes does not seem likely to significantly affect the qualitative behavior of our results.

In closing we would also like to stress that although the results presented here are strictly for a toy 4D warped flux compactification model, the methods introduced can be generalized straightforwardly to six dimensions. However, as discussed in [1], to start with the relevant heat kernel coefficient on the cone in six dimensions should be found. In addition, in the current investigation we have focused on the simplest case: a massless, minimally coupled scalar field. It should be also possible to extend our analysis to the case of a bulk scalar field with self interactions and other fields in the multiplets appearing in the supergravity model, which our model is based on. We hope to report on the results of these extended analyses in the near future.

⁶ If any terms in B_4 were incorrect then conformal invariance would be ruined.

Acknowledgements

EE was supported in part by MEC (Spain), projects PR2006-0145 and FIS2006-02842, and by AGAUR, contract 2005SGR-00790. MM was supported in part by Monbu-Kagakusho Grant-in-Aid for Scientific Research (B) No. 17340075 at the YITP and by the project ‘‘Transregio (Dark Universe)’’ at the ASC.

APPENDIX A: ASYMPTOTIC EXPANSION OF THE ZETA FUNCTION

In order to isolate the divergent behavior in the zeta function, due to small s , we need to expand Eq. (3.8). Towards this end we shall make use of the asymptotic expansion of the Hurwitz zeta function [17]:

$$\begin{aligned} \zeta_H(2s+2j-2, \frac{1}{2} + \frac{1+r}{2\kappa}n) &= \frac{1}{2s+2j-3} \left(\frac{1}{2} + \frac{(1+r)n}{2\kappa} \right)^{-(2s+2j-3)} + \frac{1}{2} \left(\frac{1}{2} + \frac{(1+r)n}{2\kappa} \right)^{-(2s+2j-3)-1} \\ &+ \frac{1}{2s+2j-3} \sum_{k=2}^{\infty} \frac{B_k}{k!} (2s+2j-3)_k \left(\frac{1}{2} + \frac{1+r}{2\kappa}n \right)^{-(2s+2j-3)-k}, \end{aligned} \quad (\text{A1})$$

where the B_k are Bernoulli numbers. Furthermore, in the limit of large n and fixed j , the asymptotic expansion of ζ_H is found to be

$$\zeta_H(2s+2j-2, \frac{1}{2} + \frac{1+r}{2\kappa}n) \left[\frac{n^2}{\kappa^2} (1-r)^2 + 1 \right]^j \simeq F(n, j; s), \quad (\text{A2})$$

where

$$F(n, j; s) := \frac{n^{-1-2s}}{\kappa^{-1-2s}} \frac{(1-r)^{2j}}{(1+r)^{1+2j+2s}} \frac{2^{-6+2j+2s}}{45(2s+2j-3)} \left(w_0 \frac{n^4}{\kappa^4} + w_2 \frac{n^2}{\kappa^2} + w_4 \right), \quad (\text{A3})$$

and we have defined

$$\begin{aligned} w_0(j, s) &= 360(1+r)^4, \\ w_2(j, s) &= \frac{360j(1+r)^4}{(1-r)^2} - 60(1+r)^2(-3+2s+2j)(-2+2s+2j), \\ w_4(j, s) &= \frac{180(j-1)j(1+r)^4}{(1-r)^4} - \frac{60j(1+r)^2(-3+2j+2s)(-2+2s+2j)}{(1-r)^2} \\ &+ 7(-3+2s+2j)(-2+2s+2j)(-1+2s+2j)(2s+2j). \end{aligned} \quad (\text{A4})$$

Note the form of these terms, especially w_4 , will be important for the analytic continuation of the zeta-function.

APPENDIX B: ANALYTIC CONTINUATION

In this appendix we discuss the analytic continuation of the various functions discussed in the main text. The expression for the analytic continuation of $\zeta(s)$ to $s \rightarrow 0$ is given by

$$\begin{aligned} \zeta(0) &= \frac{g^2}{\pi} \int d^2x \sum_{n=1}^{\infty} \left[-4 \left(\zeta_H(-2, \frac{1}{2} + \frac{1+r}{2\kappa}n) - F(n, 0, 0) \right) + \left(\zeta_H(0, \frac{1}{2} + \frac{1+r}{2\kappa}n) \left(\frac{n^2}{\kappa^2} (1-r)^2 + 1 \right) - F(n, 1, 0) \right) \right] \\ &+ \frac{\kappa g^2}{720\pi(1+r)} \int d^2x \left[\left(\frac{(1+r)^4}{\kappa^4} - \frac{(1+r)^2}{\kappa^2} - 14 \right) - \frac{(1-r)^2}{(1+r)^2} \left(\frac{3(1+r)^4}{\kappa^4} + \frac{3(1+r)^4}{(1+r)^2} \kappa^2 - 14 \right) \right] \\ &+ \sum_{j=2}^{\infty} \frac{(1-r)^{2j}}{(2j-3)(1+r)^{2j}} \left(90 \frac{(1+r)^4}{(1-r)^4} - 60 \frac{(1+r)^2}{(1-r)^2} (2j-3) + 14(2j-3)(2j-1) \right). \end{aligned} \quad (\text{B1})$$

Note that the axisymmetric modes do not contribute to $\zeta(0)$.

We next discuss the analytic continuation that is required to derive the expression for $\zeta'(0)$. The analytic continuation of $P'(s)$ to $s \rightarrow 0$ is given by

$$\begin{aligned}
P'(0) &= \frac{(2g)^2}{\pi} \left\{ \left(2 \ln(2g) - 1 \right) \sum_{n=1}^{\infty} \left[\zeta_H \left(-2, \frac{1}{2} + \frac{1+r}{2\kappa} n \right) - F[n, 0; 0] \right] \right. \\
&\quad - \frac{\ln(2g)}{2} \sum_{n=1}^{\infty} \left[\zeta_H \left(0, \frac{1}{2} + \frac{1+r}{2\kappa} n \right) \left(\frac{n^2}{\kappa^2} (1-r)^2 + 1 \right) - F[n, 1; 0] \right] \\
&\quad - \sum_{n=1}^{\infty} \left[2\zeta_{H'} \left(-2, \frac{1}{2} + \frac{1+r}{2\kappa} n \right) - \partial_s F[n, 0; s] \Big|_{s \rightarrow 0} \right] \\
&\quad + \frac{1}{4} \sum_{n=1}^{\infty} \left[2\zeta_{H'} \left(0, \frac{1}{2} + \frac{1+r}{2\kappa} n \right) \left(\frac{n^2}{\kappa^2} (1-r)^2 + 1 \right) - \partial_s F[n, 1; s] \Big|_{s \rightarrow 0} \right] \\
&\quad \left. + \sum_{j=2}^{\infty} \frac{2^{-2j}}{j(j-1)} \sum_{n=1}^{\infty} \left(\zeta_H \left(2j-2, \frac{1}{2} + \frac{1+r}{2\kappa} n \right) \left(\frac{n^2}{\kappa^2} (1-r)^2 + 1 \right)^j - F[n, j; 0] \right) \right\}. \tag{B2}
\end{aligned}$$

Note, we must also pay attention to the counterterms. The product $G(j, s)\Delta(j, s)$ can be written as

$$\begin{aligned}
G(j, s)\Delta(j, s) &= \frac{1}{2^4 \pi} \frac{\Gamma(s+j-1)}{\Gamma(s)j!} \frac{g^{2(1-s)} \kappa^{1+2s} (1-r)^{2j}}{(1+r)^{1+2s+2j}} \frac{1}{45(2s+2j-3)} \int d^2x \\
&\quad \times \left(w_0(j, s) \frac{\zeta_R(2s-3)}{\kappa^4} + w_2(j, s) \frac{\zeta_R(2s-1)}{\kappa^2} + w_4(j, s) \zeta_R(2s+1) \right), \tag{B3}
\end{aligned}$$

where, as before, we must consider the $j = 0$, $j = 1$ and $j \geq 2$ modes separately. The contribution from the $j = 0$ mode is the simplest one, and analytic continuation to $s = 0$ results in

$$\begin{aligned}
\frac{d}{ds} \left(G(0, s)\Delta(0, s) \right) \Big|_{s \rightarrow 0} &= \frac{1}{2^4 \pi} \frac{1}{135} \frac{g^2 \kappa}{(1+r)} \int d^2x \left\{ \left(-\frac{1}{s-1} - \frac{2}{2s-3} + 2 \ln \left(\frac{\kappa}{g(1+r)} \right) \right) \right. \\
&\quad \times \left(w_0(0, 0) \frac{\zeta_R(-3)}{\kappa^4} + w_2(0, 0) \frac{\zeta_R(-1)}{\kappa^2} + w_4(0, s) \zeta_R(2s+1) \Big|_{s \rightarrow 0} \right) \\
&\quad + w_0(0, 0) \frac{2\zeta_R'(-3)}{\kappa^4} + w_2'(0, 0) \frac{\zeta_R(-1)}{\kappa^2} + 2w_2(0, 0) \frac{\zeta_R'(-1)}{\kappa^2} \\
&\quad \left. + \partial_s \left(w_4(0, s) \zeta_R(2s+1) \right) \Big|_{s \rightarrow 0} \right\} \\
&= \frac{1}{2^4 \pi} \frac{1}{135} \frac{g^2 \kappa}{(1+r)} \int d^2x \left\{ \left(\frac{5}{3} + 2 \ln \left(\frac{\kappa}{g(1+r)} \right) \right) \left(3 \frac{(1+r)^4}{\kappa^4} + 30 \frac{(1+r)^2}{\kappa^2} - 42 \right) \right. \\
&\quad \left. - 50 \frac{(1+r)^2}{\kappa^2} + \frac{720(1+r)^4}{\kappa^4} \zeta_R'(-3) - \frac{720(1+r)^2}{\kappa^2} \zeta_R'(-1) + 14(11-6\gamma) \right\}, \tag{B4}
\end{aligned}$$

where we have used the fact that

$$w_4(0, s) \zeta_R(2s+1) = -42 + 14(11-6\gamma)s + O(s^2). \tag{B5}$$

Similar steps follow for the $j = 1$ mode. By setting $j = 1$ in $G(j, s)\Delta(j, s)$, differentiating with respect to s , and then taking the analytic continuation as $s \rightarrow 0$, we obtain

$$\begin{aligned}
\frac{d}{ds} \left(G(1, s)\Delta(1, s) \right) \Big|_{s \rightarrow 0} &= -\frac{1}{2^4 \pi} \frac{1}{45} \frac{g^2 \kappa (1-r)^2}{(1+r)^3} \int d^2x \left\{ \left(2 + 2 \ln \left(\frac{\kappa}{g(1+r)} \right) \right) \right. \\
&\quad \times \left(3 \frac{(1+r)^4}{\kappa^4} - 30 \frac{(1+r)^4}{\kappa^2 (1-r)^2} - 14 + \frac{60(1+r)^2}{(1-r)^2} \right) \\
&\quad - 10 \frac{(1+r)^2}{\kappa^2} + \frac{720(1+r)^4}{\kappa^4} \zeta_R'(-3) + \frac{720(1+r)^4}{\kappa^2 (1-r)^2} \zeta_R'(-1) \\
&\quad \left. - 14 - \frac{120(1+r)^2}{(1-r)^2} + \gamma \left(-28 + \frac{120(1+r)^2}{(1-r)^2} \right) \right\}, \tag{B6}
\end{aligned}$$

where we have used the expansion around $s = 0$:

$$w_4(1, s)\zeta_R(2s + 1) = -14 + \frac{60(1+r)^2}{(1-r)^2} + \left[-14 - \frac{120(1+r)^2}{(1-r)^2} + \gamma \left(-28 + \frac{120(1+r)^2}{(1-r)^2} \right) \right] s + O(s^2). \quad (\text{B7})$$

For the modes with $j \geq 2$, we obtain

$$\begin{aligned} & \sum_{j=2}^{\infty} \frac{d}{ds} \left(G(j, s) \Delta(j, s) \right) \Big|_{s \rightarrow 0} \\ &= \frac{1}{2^4 \pi} \sum_{j=2}^{\infty} \frac{1}{45j(j-1)(2j-3)} \frac{g^2 \kappa (1-r)^{2j}}{(1+r)^{1+2j}} \int d^2x \\ & \times \left\{ \left[\psi(j-1) - \frac{2}{2j-3} + 2 \ln \left(\frac{\kappa}{g(1+r)} \right) \right] \left(\frac{w_4(j, s) \zeta_R(2s+1)}{\Gamma(s)} \right) \Big|_{s \rightarrow 0} \right. \\ & + \left. w_0(j, 0) \frac{\zeta_R(-3)}{\kappa^4} + w_2(j, 0) \frac{\zeta_R(-1)}{\kappa^2} + \frac{1}{2} w_4(j, 0) + \frac{1}{2} \left(3\gamma w_4(j, 0) + \partial_s w_4(j, s) \Big|_{s \rightarrow 0} \right) \right\} \\ &= \frac{1}{2^4 \pi} \sum_{j=2}^{\infty} \frac{1}{45j(j-1)(2j-3)} \frac{g^2 \kappa (1-r)^{2j}}{(1+r)^{1+2j}} \int d^2x \\ & \times \left\{ \left[\psi(j-1) - \frac{2}{2j-3} + 2 \ln \left(\frac{\kappa}{g(1+r)} \right) \right] \right. \\ & \times 2j(j-1) \left(7(-3+2j)(-1+2j) - \frac{30(-3+2j)(1+r)^2}{(1-r)^2} + \frac{45(1+r)^4}{(1-r)^4} \right) \\ & + \frac{3(1+r)^4}{\kappa^4} + \frac{5(1+r)^2 [6+4j^2-8j^{\frac{2+r(-1+2r)}{(1-r)^2}}]}{\kappa^2} \\ & + \frac{2}{(1-r)^4} \left[-21(1-r)^4 + 84\gamma(1-r)^4 j^4 - 16j^3(1-r)^2 \left(-7(1-r)^2 + 9\gamma(3+r(-1+3r)) \right) \right. \\ & - 4j \left(-2(1-r)^2(38+r(-1+38r)) + 9\gamma(13+r(8+r(18+r(8+13r)))) \right) \\ & \left. \left. + 12j^2 \left(-(1-r)^2(31+\gamma(-22+31r)) + 4\gamma(17+\gamma(-8+r(27+r(-8+17r)))) \right) \right] \right\}, \quad (\text{B8}) \end{aligned}$$

where in the first step we used that fact that

$$\left[\frac{w_4(j, s) \zeta(2s+1)}{\Gamma(s)} \right]' = \frac{1}{2} w_4'(j, 0) + \frac{3}{2} \gamma w_4(j, 0). \quad (\text{B9})$$

APPENDIX C: CONTRIBUTION FROM THE AXISYMMETRIC MODES

The $n = 0$ mode, λ_{m0} , can be treated independently as follows. Using the binomial expansion, we straightforwardly obtain

$$\begin{aligned} \zeta_0(s) &= \int d^2x \frac{(2g)^{2(1-s)}}{2\pi(s-1)} \sum_{m=1}^{\infty} \left[\left(m + \frac{1}{2} \right)^2 - \frac{1}{4} \right]^{1-s} \\ &= \int d^2x \frac{(2g)^{2(1-s)}}{2\pi} \sum_{j=0}^{\infty} \frac{2^{-2j} \Gamma(j+s-1)}{j! \Gamma(s)} \left[\zeta_H(2s+2j-2, \frac{1}{2}) - \left(\frac{1}{2} \right)^{2(1-s-j)} \right]. \quad (\text{C1}) \end{aligned}$$

This expression requires no further regularization, because the analytic continuation is already *built-in* to this type of zeta function. The final result is

$$\zeta_0'(0) = \int d^2x g^2 \frac{\zeta_R(3)}{\pi^3}, \quad (\text{C2})$$

where we have used the fact that

$$\sum_{j=2}^{\infty} \frac{2^{-2j}}{j(j-1)} \left[\zeta_H(-2+2j, \frac{1}{2}) - \left(\frac{1}{2} \right)^{2(1-j)} \right] = \frac{1}{4} (-1 + \ln 2) + \frac{7}{8\pi^2} \zeta_R(3), \quad (\text{C3})$$

and $\zeta'_R(-2) = -\zeta_R(3)/4\pi^2$, which is derived from $\zeta_R(z) = \pi^{z-1/2}\zeta_R(1-z)[\Gamma((1-z)/2)/\Gamma(z/2)]$. An important observation is that (C2) does not agree with the corresponding expression obtained via the WKB approximation, by a factor of $-3/8$ (see equation (D36) in Ref. [1]).

-
- [1] M. Minamitsuji, W. Naylor and M. Sasaki, JHEP **0612**, 079 (2006) [arXiv:hep-th/0606238].
- [2] S. M. Carroll and M. M. Guica, arXiv:hep-th/0302067; I. Navarro, JCAP **0309**, 004 (2003) [arXiv:hep-th/0302129]; J. Garriga and M. Porrati, JHEP **0408**, 028 (2004) [arXiv:hep-th/0406158]; S. Randjbar-Daemi and V. A. Rubakov, JHEP **0410**, 054 (2004) [arXiv:hep-th/0407176]; H. M. Lee and A. Papazoglou, Nucl. Phys. B **705**, 152 (2005) [arXiv:hep-th/0407208]; S. Mukohyama, Y. Sendouda, H. Yoshiguchi and S. Kinoshita, JCAP **0507**, 013 (2005) [arXiv:hep-th/0506050].
- [3] G. W. Gibbons, R. Guven and C. N. Pope, Phys. Lett. B **595**, 498 (2004) [arXiv:hep-th/0307238]; Y. Aghababaie *et al.*, JHEP **0309**, 037 (2003) [arXiv:hep-th/0308064]; C. P. Burgess, F. Quevedo, G. Tasinato and I. Zavala, JHEP **0411**, 069 (2004) [arXiv:hep-th/0408109].
- [4] C. de Rham and A. J. Tolley, JCAP **0602**, 003 (2006) [arXiv:hep-th/0511138].
- [5] M. Peloso, L. Sorbo and G. Tasinato, Phys. Rev. D **73**, 104025 (2006) [arXiv:hep-th/0603026]; E. Papantonopoulos, A. Papazoglou and V. Zamarias, arXiv:hep-th/0611311.
- [6] B. M. N. Carter, A. B. Nielsen and D. L. Wiltshire, JHEP **0607**, 034 (2006) [arXiv:hep-th/0602086].
- [7] H. M. Lee and A. Papazoglou, Nucl. Phys. B **747**, 294 (2006) [arXiv:hep-th/0602208]; C. P. Burgess, C. de Rham, D. Hoover, D. Mason and A. J. Tolley, arXiv:hep-th/0610078.
- [8] H. Yoshiguchi, S. Mukohyama, Y. Sendouda and S. Kinoshita, JCAP **0603**, 018 (2006) [arXiv:hep-th/0512212]; Y. Sendouda, S. Kinoshita and S. Mukohyama, Class. Quant. Grav. **23**, 7199 (2006) [arXiv:hep-th/0607189]; B. Himmetoglu and M. Peloso, arXiv:hep-th/0612140.
- [9] M. R. Douglas and S. Kachru, arXiv:hep-th/0610102; F. Denef, M. R. Douglas and S. Kachru, arXiv:hep-th/0701050.
- [10] C. P. Burgess, C. Nunez, F. Quevedo, G. Tasinato and I. Zavala, JHEP **0308**, 056 (2003) [arXiv:hep-th/0305211].
- [11] K. Milton, S. D. Odintsov and S. Zerbini, Phys. Rev. **D65**, 065012 (2002).
- [12] S. L. Parameswaran, S. Randjbar-Daemi and A. Salvio, arXiv:hep-th/0608074.
- [13] C. P. Burgess and D. Hoover, arXiv:hep-th/0504004; D. Hoover and C. P. Burgess, JHEP **0601**, 058 (2006) [arXiv:hep-th/0507293];
- [14] E. Elizalde, Commun. Math. Phys. **198** (1998) 83 [arXiv:hep-th/9707257]; J. Comput. Appl. Math. **118**, 125 (2000); J. Phys. **A34**, 3025 (2001); E. Elizalde, S. Nojiri, S. D. Odintsov and S. Ogushi, Phys. Rev. **D67**, 063515 (2003).
- [15] A. Chodos and E. Myers, Phys. Rev. D **31**, 3064 (1985); A. Chodos and E. Myers, Can. J. Phys. **64**, 633 (1986); Phys. Rev. **D31**, 3064 (1985).
- [16] D. V. Vassilevich, Phys. Rept. **388**, 279 (2003) [arXiv:hep-th/0306138].
- [17] E. Elizalde, *Ten physical applications of spectral zeta functions*, Lect. Notes Phys. **M35** (Springer, Berlin, 1995); E. Elizalde *et al.*, *Zeta regularization techniques with applications* (World Scientific, Singapore, 1994)